Asian Journal of Chemistry; Vol. 24, No. 12 (2012), 5695-5698

ASIAN JOURNAL OF CHEMISTRY

www.asianjournalofchemistry.co.in

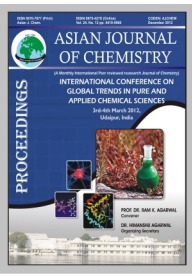

Chemical Synthesis and Structural and Magnetic Properties of Fine Grain Cobalt Substituted Lithium-Nickel-Zinc Nanostructured Ferrites†

A.T. PATHAN[1,*], M.R. BHANDARE[2], B.K. CHOUGULE[3] and A.M. SHAIKH[4]

[1]Department of Physics, M.H. Saboo Siddik College of Engineering, Mumbai-400 008, India
[2]Department of Physics, S.M.Joshi College, Hadapsar, Pune-411 028, India
[3]Ferrite Material Research Laboratory, Shivaji University, Kolhapur-416 004, India
[4]Department of Electronics, The New College, Kolhapur-416 014, India

*Corresponding author: E-mail: asrar.pathan@rediffmail.com, amshaikh7@hotmail.com

AJC-11732

A series of cobalt substituted Li-Ni-Zn ferrites with the general formula $Li_{0.5}Ni_{0.25-x/2}$ $Co_{x/2}$ $Zn_{0.5}$ Fe_2O_4 (where x = 0, 0.1, 0.2, 0.3, 0.4 and 0.5) were prepared by the novel self-propagating auto combustion method. The samples were sintered at 600 ºC before studying their structural and magnetic properties. Phase identification confirmed by XRD showed the formation of cubic spinel structure without any impurities. The average particle size calculated by Scherrer's formula and lies between 17-24 nm confirms the nano crystalline nature of the samples. The lattice parameter increases with increase of cobalt content. The dependence of porosity with cobalt content was also studied. The SEM micrographs reveal fine-grained ferrites with little agglomeration. The tetrahedral and octahedral ion complexes/ vibrations were studied by FTIR. The semiconducting behaviour of ferrite was confirmed by DC resistivity measurements. The resistivity is found to decrease with increase in temperature. The saturation magnetization (Ms), coercive field (Hc) and remanance ratio (Mr/Ms) were measured by using high field hysteresis loop tracer and their variation with composition has been studied. The saturation magnetization decreases with decreasing particle size. The decrease in magnetization results from non-magnetic layer, existing at the surface of the ferrite particles. As the particles size becomes smaller, a super paramagnetic behaviour appears.

Key Words: Auto combustion method, XRD, SEM, IR, DC resistivity, Hysteresis measurements.

INTRODUCTION

Ferrites are extensively used in magnetic recording, information storage, colour imaging, bio-processing, magnetic-refrigeration and in magneto-optical devices[1].

Magnetic particles in nano-regime is an interesting field of study because of its wide tunable applications as well as basic research understanding of fastest growing areas of researches in the field of nanotechnology[2]. Their properties are significantly modified in comparison with those of the bulk counterpart. Some new magnetic properties and phenomena, such as superp aramagnetism, spin canting and core/shell structure, are characteristics of only nanoscale magnetic materials. These properties depend on number of factors such as composition, shape, size, surface morphology, anisotropy and inter-particle interactions. Magnetic properties are sensitive to microstructure and structure parameters, which, themselves, strongly depend on the preparation method used. Consequently, different methods of preparation of nanosized powders comprise of bottom-up approach *via* sol-gel, micro-emulsion, hydrothermal, chemical co-precipitation[3] or top-down approach like ball milling[4] and high temperature sintering. Each technique has their own merits and demerits interms of tunable micro and macro scale structural and magnetic properties.

Most of these methods cannot be applied to a large scale and economic production because they require expensive and toxic reagents, complicated synthetic steps, high reaction temperature and long reaction time. Among many preparation techniques, chemical methods stand out as an alternative and highly promising method of preparation. This method is quite simple, fast and inexpensive since it does not involve intermediate decomposition and do not need calcining steps. Moreover, it controls the stoichiometry and crystallites size, which have important effect on the magnetic properties of ferrite[5].

Nano ferrites of $Li_{0.5}Ni_{0.25-x/2}$ $Co_{x/2}$ $Zn_{0.5}$ Fe_2O_4, have technological importance as they can play a role in the miniaturization

†Presented at International Conference on Global Trends in Pure and Applied Chemical Sciences, 3-4 March, 2012; Udaipur, India

process of several microwave components. Lithium ferrite possesses several attractive features: its high Curie temperature, high saturation magnetization and hysteresis loop properties offer many advantages over other spinel ferrites traditionally used in the field of microwave and memory core applications[6]. The substitution of other 3*d* ions for iron in ferrite, such as Ni, Cr, Mn or Co, plays an important role on the modifications of microstructure, as well as on the electrical and magnetic properties of lithium ferrite[7,8]. Tawfik has reported the electro-mechanical properties of $CoFe_2O_4$ ferrite transducer[9]. Bhavikatti *et al.*, have reported high coercivity for cobalt ferrite to be 272.73 Oe[10]. Ahmed *et al.* studied the enhancement of the crystal size and magnetic properties of Mg substituted Co ferrite[11]. Sattar and others have shown that Ca-substitution slightly increases the lattice parameter, the coercivity and the squareness in the Li-Zn ferrite[12]. Craus *et al.* shows that the magnetization, coercive field and lattice constant are changing *vs.* milling time and chemical composition in $LiCuFe_2O_4$ ferrites[13]. Yang *et al.* show a super-paramagnetic behaviour appears in Li-Cr ferrites as saturation magnetization decreases with particle size[14].

The present work reports the influence of Co^{2+} ions on structural behaviour and magnetic properties of Li-Ni-Zn ferrites.

EXPERIMENTAL

Mixed Co-Li-Ni-Zn ferrites having the general formula $Li_{0.5}Ni_{0.25-x/2}$ $Co_{x/2}$ $Zn_{0.5}$ Fe_2O_4 (where x = 0, 0.1, 0.2, 0.3, 0.4 and 0.5) were prepared using auto combustion method as reported in our earlier communication[15]. The powder was pre-sintered at 400 ºC for 6 h and cooled slowly to room temperature. The pre-sintered samples were ground and pressed into a disk shaped pellets of 10 mm diameter. A small quantity of polyvinyl alcohol as a binder was added to the powder. The samples were sintered again at 600 ºC for 6 h and slowly cooled at the rate of 2 ºC/min. XRD studies were done by using X-ray diffractometer (Model Philips PW 3710) using CuK_α radiation and EDX studies were done using (Model Thermo Noran NSS 200) to study the structure of powder material and the presence of elements. SEM micrograph of nano ferrite materials were recorded using a scanning electron microscope (Model Hitachi S3400N) to estimate the nanosize of the material particles. Infrared absorption spectra in the wave number range 800 to 300 cm^{-1} were recorded at room temperature by using Perkin-Elmer IR spectrometer (spectrum 100) in KBr medium. The hysteresis loop tracer was used for magnetic measurements. The saturation magnetization, coercivity and remanent magnetization were found from hysteresis loop.

RESULTS AND DISCUSSION

X-Ray diffraction: The XRD patterns of the samples with x = 0, 0.1, 0.2, 0.3, 0.4 and 0.5 are shown in Fig. 1. The pattern indicates well-defined peaks of crystalline FCC phase which confirm spinel cubic structure of the samples. No additional impurity reflections were observed ensuring the phase purity. The crystallite size of the samples was calculated using Scherrer formula[16] are listed in Table-1. Fig. 2 shows the variation of lattice constant with Co content. It is observed that the lattice parameter determined from the XRD data showed variation with composition. The lattice constant shows a linear increase with increasing cobalt content. These variations in lattice constant can be explained on the basis of lattice expansion. If the radius of doping ion is larger than the displaced ion the lattice expands and lattice constant increases. Reverse will hold if a smaller doping ion replaces a metal ion of the regular site. In the present case the lattice constant increases from 8.352 Å for x = 0 to 8.348 Å for x = 0.5. The increase in lattice constant is due to the substitution of Co^{2+} ions having larger ionic radius (0.82 Å) for Ni^{2+} ions having smaller ionic radius (0.69 Å)[17]. An increase in lattice parameter is therefore expected as observed.

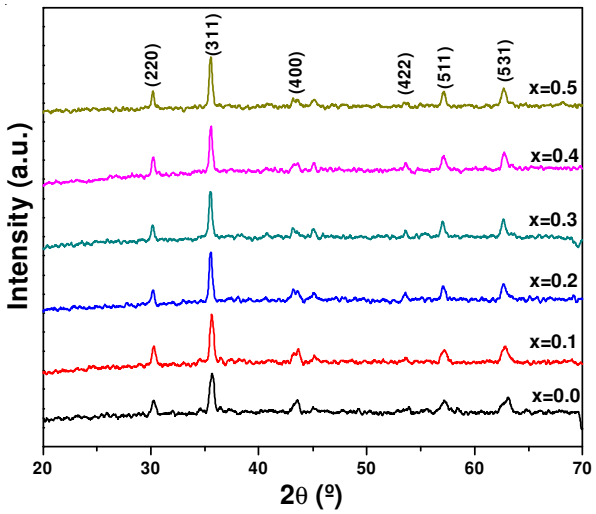

Fig. 1. X-ray diffraction patterns of $Li_{0.5}Ni_{0.25-x/2}$ $Co_{x/2}$ $Zn_{0.5}$ Fe_2O_4 ferrite samples (x = 0, 0.1, 0.2, 0.3, 0.4 and 0.5)

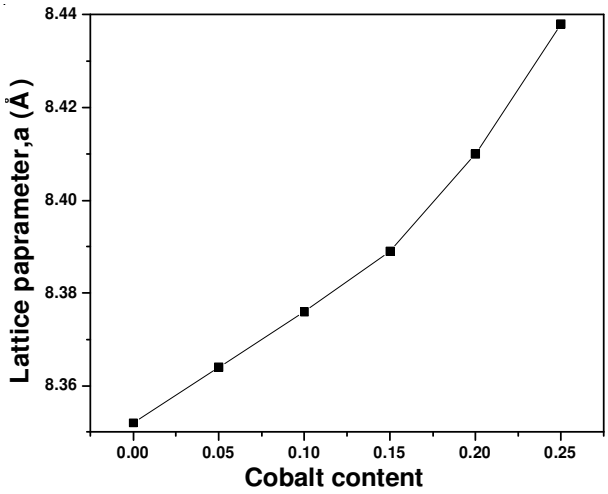

Fig. 2. Variation of lattice parameter 'a' with cobalt content

TABLE-1
DATA ON PARTICLE SIZE, LATTICE PARAMETERS AND X-RAY DENSITY

Sample	Co content	Lattice parameter a (Å)	Particle size (D, nm)	X-ray density (Gm/cm^3)
X = 0.0	0.00	8.352	17	5.167
X = 0.1	0.05	8.364	21	5.145
X = 0.2	0.10	8.376	23	5.123
X = 0.3	0.15	8.389	24	5.100
X = 0.4	0.20	8.410	24	5.035
X = 0.5	0.25	8.438	23	5.018

SEM analysis: Fig. 3. shows the SEM micrograph of the sample with x = 0, 0.1, 0.2, 0.3, 0.4 and 0.5 it is observed that the majority of the grains are spherical in shape. The mechanical behaviour and physical properties of materials are strongly influenced by their microstructure. Thus microstructure studies are essential in order to understand the relationship between the processing parameter and the behaviour of the materials used in practical applications.

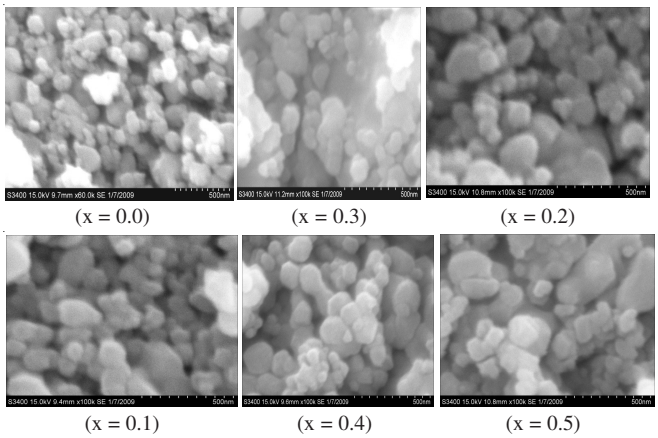

Fig. 3. SEM images of $Li_{0.5}Ni_{0.25-x/2}$ $Co_{x/2}$ $Zn_{0.5}$ Fe_2O_4 ferrite samples (x = 0, 0.1, 0.2, 0.3, 0.4 and 0.5)

The microstructure of the sample depends on the Co content. The SEM micrograph for x = 0.0 shows well dispersed grains with identical shape and size. It is interesting to note that, as the amount of Co^{2+} content increases, the nature of the microstructure gets modulated. In the case x = 0.1 the grains are non identical in size and shape whereas for the case of x = 0.5 the grains are agglomerated.

The surface morphology of all the composition shows that the grain size increases with increase in cobalt concentration from 0.93 to 1.2 μm. The increase in grain size with cobalt content is due to the higher atomic mobility of cobalt ions[18]. On substitution of cobalt the grain texture turns to polyhedral with lesser microstructure homogeneity and a variation in grain size also observed which gradually increases with increase in cobalt concentration.

EDX analysis: The EDX spectra obtained from the centre of grain boundary indicated the presence of mainly Zn, Fe and oxygen along with small amount of Co. Table-2 shows the mass contents of individual ions in the prepared Co-Li-Ni-Zn nanostructured ferrites determined by EDX analysis.

TABLE-2
MASS CONTENTS OF INDIVIDUAL IONS IN Co-Li-Ni-Zn NANOSTRUCTURED FERRITES AS DETERMINED BY EDX ANALYSIS

Sample	Content wt. (%)					
	Li	Ni	Co	Zn	Fe	O
X = 0	0.00	8.13	0.00	17.35	60.87	13.65
X = 0.1	0.00	4.60	1.37	17.31	60.48	16.24
X = 0.2	0.00	3.97	2.70	14.93	62.06	16.33
X = 0.5	0.00	*0.03*	8.54	13.94	57.64	19.85

The EDX results show significantly higher content of Fe relative to the formula calculated from the batch composition. The observed differences exceed the expected error of the chemical analysis expected from semi-quantitative EDX measurements significantly. The excess of iron should be manifested in the structural analysis as the second phase aside the spinel one. However, the result of above mentioned XRD analysis has shown cubic spinel structure only. Lithium is not included as it cannot be observed by EDX. Since EDX analyses were measured locally on particular crystal particles, we can conclude that part of bivalent metal ions was not incorporated into the crystalline ferrite phase during the synthesis procedure. In any case, we just would like to emphasis that the increase of Co contents causes an adequate decrease of Ni and Zn ions[19].

FTIR study: The study of infrared spectrum is an important tool to get information about the position of the ions in the crystal through the crystals vibrational modes. With a view to study the effect of dependence of normal modes and their frequency on change of the substitution of ions in Li-Zn ferrites. FTIR frequency data for the respective sites are analyzed using the FTIR spectra. The higher frequency band (ν_1) (600 cm^{-1}) and lower frequency band (ν_2) (400 cm^{-1}) are assigned to the tetrahedral and octahedral complexes[20]. It explains that the normal mode of vibration of tetrahedral cluster is higher than that of octahedral cluster. It should be attributed to the shorter bond length of tetrahedral cluster and longer bond length of octahedral cluster[21].

Magnetic measurements: Table-3 lists the magnetic measurement data, which shows that the dependence of the saturation magnetization (Ms) on the average particle size of $Li_{0.5}Ni_{0.25-x/2}$ $Co_{x/2}$ $Zn_{0.5}$ Fe_2O_4 ferrite. It can be seen that Ms decreases with decreasing particle size. When the particles are smaller, the surface effects are more dominant and these affect the magnetic properties significantly. The relation between saturation magnetization Ms of ferrite and the particle size determined from the line width of the (311) d-spacing is shown in Fig. 4. The Ms of the ferrite is found to decrease linearly with decreasing particle size. The cause of the decrease in Ms may be due to surface effect and size effect, which results in magnetic degradation of the surface and dependence on surface anisotropy energy of the ferrite, also due to existence of non-magnetic layer. Mollard reported that there are O^{2-} and OH^- ions on the surface of the ferrite, so that some amount of Fe^{2+} are oxidized to Fe^{3+} ions, which results in a decrease in Ms of γ-Fe_2O_3[22]. The adsorption of water and chemical reaction on the surface may result in the decrease of the saturation magnetization.

Fig. 5 shows variation of saturation magnetization with content of cobalt. From figure it is clear that the saturation magnetization of the samples increases with increase in the cobalt content concentration. This may be due to low orbital contribution of cobalt ions to the magnetic moment, this gives low induced anisotropy.

TABLE-3
MAGNETIC MEASUREMENT DATA

	x = 0	x = 0.1	x = 0.2	x = 0.4
Ms (emu/gm)	33.76	56.15	70.07	71.24
n_B	1.37	2.27	2.84	2.89
Particle size (D, nm)	17.00	21.00	23.00	24.00
Mr (emu/gm)	9.56	17.85	0.73	0.022
Hc (Oe)	193.3	192.69	139.5	134.69

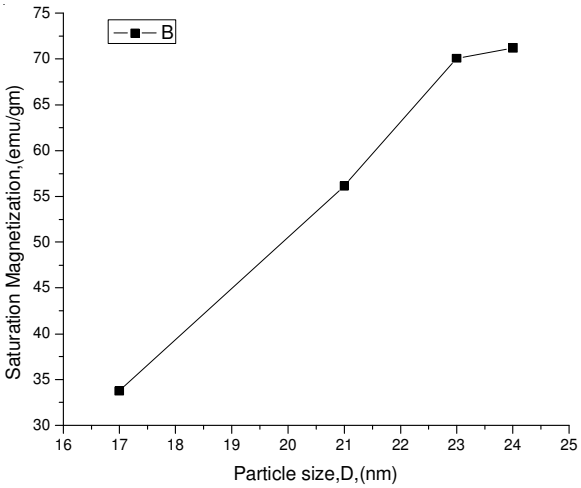

Fig. 4. Variation of saturation magnetization with particle size

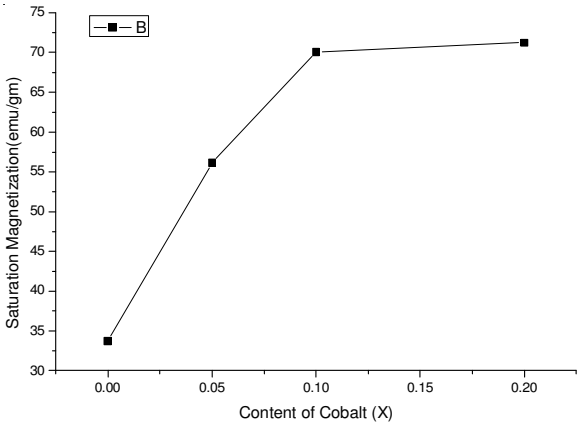

Fig. 5. Variation of saturation magnetization with content of cobalt

The experimental magnetic moment was calculated using the following relation[19].

$$n_B = [Mw \times Ms]/5585$$

where, Mw is the molecular weight of the sample and Ms is the saturation magnetization in emu/gm obtained from the hysteresis data. In Fig. 6 we can see an increase in Magnetic moment with content of cobalt.

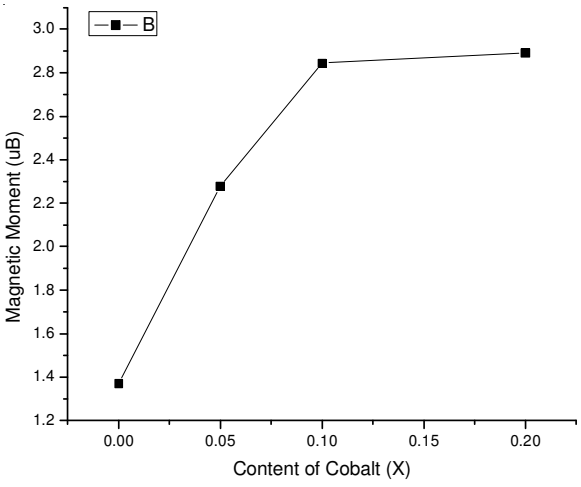

Fig. 6. Variation of Bohr Magnetron with content of cobalt

It is reported that in the conventional Ni-Zn ferrite processing procedure, Fe^{2+} ions are believed to be introduced due to the following reasons: (i) volatilization of Co atoms and (ii) oxidation/reduction (heating/cooling cycles). The result reported in this paper clearly indicate that at least the charged cations interact to a limited extent to create a finite, nonzero disorder locally, which can significantly alter the magnetic properties. The significant differences in magnetic moment values could have arisen from the local sub lattice nonstoichiometries. At this point, the exact nature of such interactions is only hypothetical and is being studied[23].

Conclusion

Single phase spinel ferrites of Co-substituted Li-Ni-Zn ferrites are studied. The Co substitution slightly increases the lattice parameter and particle size. The saturation magnetization decreases with decreasing particle size because of surface effect and size effect. As the particle size decreases, a super para-magnetic behaviour appears. IR study shows two strong bands as an essential feature of spinel ferrites with a slight shift in band positions owing to change in cobalt concentration.

REFERENCES

1. S. Ghatak, A.K. Meikap, M. Sinha and S.K. Pradhan, *Mater. Sci. Appl.*, **1**, 177 (2010).
2. K. Parekh, *Ind. J. Pure and Appl. Phys.*, **48**, 581 (2010).
3. C.H. Chia, S. Zakaria, M. Yusoff, S.C. Goh, C.Y. Haw, Sh. Ahmadi, N.M. Huang and H.N. Lim, *Ceram. Int.*, **36**, 605 (2010).
4. J.D. Fatemi, G.V. Harris, M.V. Browning and P.J. Kirkl, *J. Appl. Phys.*, **83**, 6867 (1998).
5. M.A. Ahmed, N. Okasha and S.I. EI-Dek, *Ceram. Int.*, **36**, 1529 (2010).
6. R.G. Kharabe, S.A. Jadhav, A.M. Shaikh, D.R. Patil and B.K. Chougule, *Mater. Chem. Phys.*, **72**, 77 (2001).
7. A. Pradeep, C. Thangasamy and G. Chandrasekaran, *J. Mater. Sci*., **15**, 797 (2004).
8. H.M. Vidatallah, C. Jhonson, F. Berry and M. Pekala, *Solid State Commun.*, **120**, 171 (2001).
9. A. Tawfik, *J. Magn. Magn. Mater.*, **237**, 283 (2001).
10. A.M. Bhavikatti, S. Kulkarni and A. Lagashetty, *Int. J. Elect. Eng. Res.*, **2**, 125 (2010).
11. M.A. Ahmed and A.A. El-Khawlani, *J. Magn. Magn. Mater.*, **321**, 1959 (2009).
12. A.A. Sattar, H.M. EI-Sayed and W.R. Agami, *J. Mater. Eng. Perform.*, **16**, 573 (2007).
13. M.L. Craus, V. Dobrea, S. Predenau and C. Neculita, *J. Optoelec. Adv. Mater.*, **4**, 329 (2002).
14. H. Yang, L. Shen, L. Zhao, L. Song, J. Zhao, Z. Wang, L. Wang and D. Zhang, *Mater. Lett.*, **57**, 2455 (2003).
15. M.R. Bhandare, H.V. Jamadar, A.T. Pathan, B.K. Chougule and A.M. Shaikh, *J. Alloys Compds.*, **509**, L113 (2011).
16. B.D. Cullity and S.R. Stock, Elements of X-ray Diffraction, Prentice-Hall, Englewood Cliffs. NJ, edn. 3, 170 (2001).
17. T. Ahmed, I.Z. Rahman and M.A. Rahman, *J. Mater. Sci. Technol.*, **797**, 152 (2004).
18. E. Rezlescu, L. Sachelarie, P.D. Popa and N. Rezlescu, *IEEE Trans. Mag.*, **36**, 3962 (2000).
19. M. Usakova, J. Lukas, R. Dosoudil and J. Subrt, *J. Mater. Sci.: Mater. Electron.*, **18**, 1183 (2007).
20. B.K. Labde, C.M. Sable and N.R. Shamkuwar, *Mater. Lett.*, **57**, 1651 (2003).
21. V. Naidu, S.K.A. Ahmed, M.S. Dawood and M. Suganthi, *Int. J. Comp. Appl.*, **24**, 18 (2011).
22. H. Yang, Z. Wang, M. Zhao, J. Wang, D. Han, H. Luo and L. Wang, *Mater. Chem. Phys.*, **48**, 60 (1997).
23. R. Peelamedu, C. Grimes, D. Agrawal and R. Roy, *J. Mater. Res.*, **18**, 2292 (2003).